Transfer of exosomal microRNAs confers doxorubicin resistance in osteosarcoma cells

TAO CAI[1,2], CHUNLIN ZHANG[1] and TAICHEN ZHAN[1]

[1]Department of Orthopedic Surgery, Shanghai Tenth People's Hospital Affiliated to Tongji University;
[2]Department of Orthopedic Surgery, Tongji Hospital Affiliated to Tongji University,
Tongji University School of Medicine, Shanghai 200072, P.R. China

Received April 14, 2021; Accepted July 19, 2022

DOI: 10.3892/mmr.2023.12973

Abstract. Osteosarcoma (OS) is the commonest primary malignant bone tumor in children and adolescents. However, chemotherapy resistance is a major challenge for the treatment of OS. Exosomes have been reported to serve an increasingly important role in different stages of tumor progression and chemotherapy resistance. The present study investigated whether exosomes derived from doxorubicin-resistant OS cells (MG63/DXR) could be taken up in doxorubicin-sensitive OS cells (MG63) and induce a doxorubicin-resistant phenotype. MDR-1, as the specific mRNA of chemoresistance, can be transferred by exosomes from MG63/DXR cells to MG63 cells. In addition, the present study identified 2,864 differentially expressed miRNAs (456 upregulated and 98 downregulated with fold-change >2.0, $P<5x10^{-2}$, and FDR<0.05) in all three sets of exosomes from MG63/DXR cells and MG63 cells. The related miRNAs and pathways of exosomes involved in the doxorubicin resistance were identified by bioinformatic analysis. A total of 10 randomly selected exosomal miRNAs were dysregulated in exosomes from MG63/DXR cells relative to MG63 cells by reverse transcription-quantitative PCR detection. As a result, miR-143-3p was found high expressed in exosomes from doxorubicin-resistant OS cells compared with doxorubicin-sensitive OS cells and upregulation of exosomal miR-143-3p abundance associated with the poor chemotherapeutic response to OS cells. Briefly, transfer of exosomal miR-143-3p confers doxorubicin resistance in osteosarcoma cells.

Introduction

Osteosarcoma (OS) is the commonest primary malignant bone tumor in young patients. Although, with the development of surgical skills and the application of neoadjuvant chemotherapy, the 5-year survival rate of patients has increased to 70%, there are still a number of challenges that physicians face in OS, including the chemoresistance, local recurrence and pulmonary metastasis (1,2). The most important prognostic indicator for OS patients is the necrosis of OS after chemotherapy before operations. Patients with <90% tumor necrosis, who are considered as chemoresistant to the agents, will have poor outcomes in the future (3). Unfortunately, >70% of patients are insensitive to chemotherapeutic agents and the chemoresistance appears to be mediated by a variety of mechanisms (4).

Exosomes are a class of 30- to 150-nm extracellular vesicles (EVs) generated by almost all cell types, including cancer cells (5). Exosomes, with lipid bilayer membranes, can be taken up by neighboring or distant recipient cells and exosomal contents, including small RNA and protein, can exhibit biological activities such as immunomodulation (6), autophagy (7), stem cell differentiation (8) and intercellular communication (9), which is known as the third method of cellular communication. Exosomal miRNAs, protected by lipid membranes of exosomes from being digested by RNases, can be stably transferred between two different tumor cells and participate in tumor progression (9). Some related research about the function of cell-secreted exosomal miRNAs (exo-miRNAs) in growth, metastasis, angiogenesis and multidrug resistance (MDR) for malignant tumors has been reported (10). However, the importance of exosomes and related exo-miRNAs in the pathogenesis of the OS cells has yet to be established. The present study investigated the potential influence of exosomes from doxorubicin-resistant OS cells in the proliferation, migration, invasion and MDR on the doxorubicin-sensitive OS cells and searched for potential differentially expressed exo-miRNAs that would predict the different response to chemotherapy.

Methods and materials

Cell culture and reagents. A total of four OS cell lines, MG63 cells (doxorubicin-sensitive OS cells), doxorubicin-resistant MG63 cells (MG63/DXR), KHOS cells (doxorubicin-sensitive OS cells) and doxorubicin-resistant KHOS cells (KHOS/DXR), were chosen in the present study and purchased from the American Type Culture Collection. All four cell lines were

Correspondence to: Dr Chunlin Zhang, Department of Orthopedic Surgery, Shanghai Tenth People's Hospital Affiliated To Tongji University, Tongji University School of Medicine, 301 Yanchang Zhong Road, Shanghai 200072, P.R. China
E-mail: shzhangchunlin123@163.com

Key words: osteosarcoma, exosome, microRNA, chemoresistance

cultured in DMEM (Gibco; Thermo Fisher Scientific, Inc.) containing 10% FBS depleted of exosomes (FDE; ScienCell Research Laboratories, Inc.) and 1% penicillin/streptomycin (Gibco; Thermo Fisher Scientific, Inc.). All of the cells were cultured in a humidified incubator with 5% CO_2 at 37˚C. When the cell density reached 70-80%, the conditioned medium was collected.

Exosome isolation. After the collection of the conditioned medium from OS cells, the supernatant was collected and centrifuged as follows: 300 x g for 10 min to remove cells, 2,000 x g for 10 min to remove dead cells, 10,000 x g for 30 min to remove cell debris, 100,000 x g for 70 min to collect pellets, washed with PBS and 100,000 x g for 70 min to collect exosomes all at 4˚C. NanoSight particle tracking analysis (NTA) was conducted to identify the concentration and number of exosomes and the bicinchoninic acid (BCA) method (Thermo Fisher Scientific, Inc.) was applied to examine the exosomal protein concentration.

Transmission electron microscopy (TEM). For TEM observation, 10 μl of exosome solution was placed onto copper mesh and incubated at room temperature for 10 min. After that, the copper mesh was washed with sterile distilled water and 10 μl of 2% uranyl acetate was pipetted on the copper mesh for negative staining for 1 min, the excess fluid was removed and the mesh was dried under an incandescent lamp for 2 min. Finally, the copper mesh was observed under a transmission electron microscope at 80 KV (JEOL, Ltd.).

NTA. After the isolation of the exosomes from OS cells, PBS was used to dilute at a factor of 100 or 1,000 for exosomes to obtain an approximate number of vesicles prior to NTA. ZetaView PMX 110 (Particle Metrix GmbH) and its corresponding software (ZetaView 8.02.28) were applied to analyze the size and concentration of the exosomes from OS cells.

Western blot analysis. Total protein was isolated using cell lysis buffer and the bicinchoninic acid (BCA) method (Thermo Scientific, Inc.) was applied to examine the exosomal protein concentration as described before. The densitometry of the protein was detected by NanoDrop-1000 (Thermo Scientific, Inc. USA) with the software Nanodrop 3.3.0 by the BCA method. The equal amounts of protein (50 μg per lane) were loaded for western blot analysis. To identify the three specific proteins, CD9 (23 kDa), CD63 (26 kDa), and TSG-101 (72 kDa) were positive experssed, exosomes were collected and lysed using RIPA protein extraction reagent (Beyotime Institute of Biotechnology) supplemented with a protease inhibitor cocktail (Roche Applied Science). Proteins were loaded onto 10% SDS-PAGE gels for electrophoresis, transferred to PVDF membranes and blocked in 5% milk for 1 h at 4˚C overnight prior to incubation with the indicated primary antibodies for 3 h at room temperature. After washing with trisbuffered saline with 0.1% Tween 20 (TBST) four times, the secondary antibodies were incubated with the membrane at room temperature for 1.5 h. The antibodies used in the experiments included anti-CD63 (1:1,000; Santa Cruz Biotechnology, Inc.), anti-CD9 (1:1,000; Santa Cruz Biotechnology, Inc.), anti-TSG101 (1:1,000; Santa Cruz Biotechnology, Inc.) and anti-β-actin (1:1,000; Santa Cruz Biotechnology, Inc.). All experiments were repeated three times. The bound antibodies were visualized with Pierce ECL Western Blotting Substrate (Thermo Fisher Scientific). Image pro-Plus 6.0 (Media Cybernetics, Inc.) was used for the densitometry of the brands.

Exosome labeling and uptake. MG63 cells were stained with the CellTrace CFSE Cell Proliferation kit (Invitrogen; Thermo Fisher Scientific, Inc.) according to the manufacturer's instructions and exosomes were labeled using the PKH67 Blue Fluorescent Cell Linker kit (MINI67-1KT; MilliporeSigma). PKH67 dye solution (1 ml; 1:1,000) was mixed with 20 μg of exosomes for 20 min at 36.5˚C, washed with PBS and centrifuged at 100,000 x g for 70 min at 4˚C. PKH67-labeled exosomes (4 μg) were resuspended in IMDM supplemented with 10% FDE and added to MG63 cells at 36.5˚C. The cells were washed and fixed in 3.7% PFA for 10 min to stop the process of uptake with different time of incubation. Then, the cells were stained with fluorescein isothiocyanate (FITC)-conjugated phalloidin (MilliporeSigma) and the uptake of exosomes at different time points was observed under a confocal fluorescence microscope (Nikon Eclipse E800M; Nikon Corporation).

Cell viability. Cell viability was evaluated by the CellTiter-Glo 2.0 Reagent (cat. no. G7572; Promega Corporation). MG63 cells were seeded at a density of $2x10^3$ cells/well in 96-well flat-bottomed tissue culture plates in the presence of DMEM +10% FDE and test compound at room temperature for approximately 30 min. Then, 100 μl of CellTiter-Glo 2.0 Reagent was added and the content was mixed for 2 min on an orbital shaker. After incubating the plate at room temperature for 10 min, the luminescence was recorded.

Cell migration assay. Transwell experiment was conducted for the migration assay. OS cells were seeded at a density of $1.2x10^5$ cells/well in 24-well plates with 500 μl of cell culture medium for 48 h. Then the MG63 cells were fixed with 500 μl of 4% paraformaldehyde at room temperature for 15 min. After washing with deionization water for 3 to 5 times, the OS cells were observed under a microscope. Experiments were performed at least three times and the results were recorded as the mean of these experiments.

Cell invasion assay. MG63 cells were seeded at the destiny of $2.0x10^5$ cells/ml in 24-well plates and incubated with exosomes from MG63/DXR (Exo-MG63-DXR; 100 μl/ml) for 48 h at 36.5˚C. Matrigel (cat. no. 356235; Corning, Inc.) was thawed on a shaker at 4˚C for 2 h. Matrigel (10 μl) was added the cell pellet in an Eppendorf tube and mixed gently. Cells that were mixed with cold Matrigel were gently pipetted into the middle of a well in a 24-well plate into a drop-like shape. The Matrigel drops are solidified in a 37˚C incubator with 5% CO_2 injection for 20 min. The cells were digested and centrifuged with the speed of 200 x g for 5 min at room temperature. After termination of digestion, the cells washed twice with PBS, and resuspended in 10 g/l BSA. The cells were seeded at a density of $1.2x10^5$ cells/well in 24-well plates. Doxorubicin (100 ng/ml) was added into the treated MG63 cells for 24 h and the cells were fixed with 500 μl of 4% paraformaldehyde

Table I. Sequences of all miRNA mimics, mimic NC, miRNA inhibitors and inhibitor NC.

miRNA	Sequence
miRNA inhibitor NC	CAG UAC UUU UGU GUA GUA CAA
miRNA mimic NC	UUC UUC GAA CGU GUC ACG UTT
	ACG UGA CAC GUU CGG AGA ATT
miRNA-143-3p inhibitor	GAG CUA CAG UGC UUC AUC UCA
miRNA-143-3p mimic	UGA GAU GAA GCA CUG UAG CUC
	GCU ACA GUG CUU CAU CUC AUU
miRNA-493-5p inhibitor	AAU GAA AGC CUA CCA UGU ACAA
miRNA-493-5p mimic	UUG UAC AUG GUA GGC UUU CAUU
	UGA AAG CCU ACC AUG UAC AAUU
miRNA-494-3p inhibitor	UGA AAC AUA CAC GGG AAA CCU UCU
miRNA-494-3p mimics	UGA AAC AUA CAC GGG AAA CCU CU
	AGG UUU CCC GUG UAU GUU UCA UU

miRNA, microRNA; NC, negative control.

at room temperature for 15 min. The chamber in the control group was treated with 500 μl crystal violet staining solution for 20 min at room temperature (control group). After washing with deionized water 3-5 times, the tumor cells were observed under a confocal microscope (LSM 900; Carl Zeiss AG) with magnification x400. Experiments were performed at least three times and the results were recorded as the mean of these experiments.

RNA sequence and reverse transcription-quantitative (RT-q) PCR. Exosomal RNAs were extracted using TRIzol® (Thermo Fisher Scientific, Inc.) according to the manufacturer's instructions and miRNAs were extracted by the RNeasy/miRNeasy Mini kit (Qiagen, Inc.). The amount and quality of small RNAs in the total RNAs were tested by Heyuan Biotechnology (Shanghai) Co., Ltd. Small RNA library construction and sequencing were performed by Heyuan Biotechnology (Shanghai) Co., Ltd. Then, the cDNA library was sequenced on an Illumina Hiseq 2500 (Illumina, Inc.). Raw reads were collected using related Illumina analysis software and RT-qPCR was performed on a CFX96 Real-Time System (Bio-Rad Laboratories, Inc.) using iTaq Universal One-Step RT-qPCR kits (Bio-Rad Laboratories, Inc.). The PCR cycling conditions were: 94˚C for 5 min, 94˚C for 1 min, 55˚C for 40 sec, 72˚C for 50 sec, 72˚C for 7 min and the temperature lowered to 4˚C at the end of each cycles. The cycles were repeated 29 times. The probes and primers by a web based assay design software (Probe Finder https://www.roche-applied-science.com) to identify the expression of MDR-1 (MDR-1-f 5'-GCC ATCAGTCCTGTTCTTGG-3'; MDR-1-r 5'-GCTTTTGCA TACGCTAAGAGTTC-3') and the results were expressed as the ratio between the MDR-1 and GAPDH according to the $2^{-\Delta\Delta Cq}$ method. RT-qPCR was repeated three times (11).

Micro (mi)RNA mimic and inhibitor transfection. MG63 cells and KHOS cells ($4x10^4$ cell/ml) were transfected with 100 nM of the exosomal miRNA mimic (0.16 μM/μl) [Heyuan Biotechnology (Shanghai) Co., Ltd.] and MG63/DXR and KHOS/DXR were transfected with 100 nM of the exosomal miRNA inhibitor (0.16 μM/μl) [Heyuan Biotechnology (Shanghai) Co., Ltd.] using Lipofectamine® 2000 (Invitrogen; Thermo Fisher Scientific, Inc.). PBS was used as the negative control (NC). The negative control inhibitor and mimic of the exosomal miRNAs were used for corresponding negative controls (NC; Table I). The OS cells ($4x10^4$ cell/ml) were seeded in 96-well, flat, clear-bottomed, opaque wall microplates and treated with miRNA mimic or inhibitor (0.16 μM/μl) for 48 h at the temperature of 36.5˚C. After 48 h of transfection, the four OS cells ($4x10^4$ cell/ml) were treated with doxorubicin (100 ng/ml) for another 24 h at 36.5˚C. The effect of exosomal RNAs on the viability of OS cells was determined using CellTiter-Glo Luminescent Cell Viability Assay (Promega Corporation) according to the manufacturer's instructions. The total ATP content as an estimate of total number of viable cells was measured on an automatic Fluoroskan Luminometer (Thermo Fisher Scientific, Inc.).

Bioinformatic analysis of the exosomal miRNAs. According to the exosomal miRNA sequences of MG63 and MG63/DXR, Gene Ontology (GO) analysis of target genes were conducted using the DAVID database (https://david.ncifcrf.gov/) and the pathway enrichment analysis for related.

Statistical analysis. The expression levels of exosomal miRNA from RNA sequence were analyzed by SDS software version 2.2.2 (Applied Biosystems; Thermo Fisher Scientific, Inc.). R software for Windows 4.1.2 (https://www.r-project.org/) and RStudio (https://www.rsrudio.com/products/rstudio/download) were used to draw a heatmap of differentially expressed exosomal miRNAs and between-group statistical analysis. The results are presented as the mean ± standard deviation. Statistical significance between two groups was determined using a two-tailed Student's t test. P-values were either listed or represented by the following number of asterisks: $^{*}P<5x10^{-2}$; $^{**}P<1x10-2$; $^{***}P<1x10-3$. P<5x10-2 was considered to indicate a statistically significant difference.

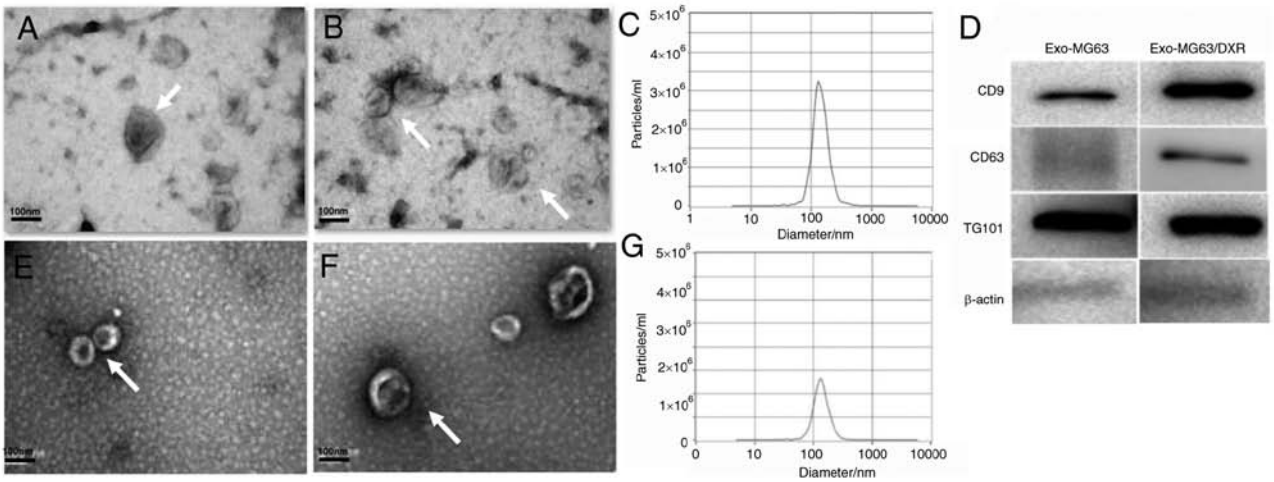

Figure 1. Isolation and identification of exosomes for MG63/DXR cells and MG63 cells. (A and B, E and F) The vesicles (arrowed) exhibited a cup shape with bilayered membranes and the diameter generated from MG63/DXR and MG63 ranged from 30-150 nm under the transmission electron microscope (scale bar=100 nm). (C and G) NanoSight particle tracking analysis identified that the predominant size of the vesicles generated from MG63/DXR and MG63 was 136.3 and 132.4 nm and the concentrations were $3.1x10^6$ particles/ml and $2.6x10^6$ particles/ml. (D) The exosomal markers CD9, CD63 and TSG101 were detected in the exosomes by western blot analysis.

Results

Isolation and identification of exosomes. First, the exosomes of the MG63 cells and MG63/DXR cells were isolated and under the TEM, the vesicles from the OS cells exhibited a cup shape with bilayered membranes and a diameter ranging from 30-150 nm (Fig. 1A and B, E and F). The main size of the vesicles was 132.4 and 136.3 nm and the concentrations were $2.6x10^6$ particles/ml and $3.1x10^6$ particles/ml for MG63 and MG63/DXR cells respectively as identified by NTA (Fig. 1C and G). In addition, the exosomal markers CD9, CD63 and TSG101 were detected by western blot analysis (Fig. 1D). Vesicles isolated from MG63 cells and MG63/DXR cells displayed typical characteristics of exosomes and MG63/DXR cells secreted more exosomes than MG63 cells.

Exosomes labelling and uptake. To examine whether exosomes from MG63/DXR (Exo-MG63/DXR) could be taken up in MG63 cells, PKH67-labeled Exo-MG63/DXR were incubated with MG63 cells and examined using fluorescence microscopy. After 3 h of incubation, the PKH67 signal was detected in the perinuclear region and an increasing PKH67 signal was observed in the perinuclear region of MG63 cells 6 and 12 h later (Fig. 2A). The results suggested that the Exo-MG63/DXR was assimilated and internalized by MG63 cells following incubation.

Influence of Exo-MG63/DXR for MG63 cells on the proliferation, invasion and migration after treatment with doxorubicin. To investigate the influence of Exo-MG63/DXR on the proliferation of MG63 cells to doxorubicin, cell viability was examined in MG63 cells in the presence of increasing concentrations of doxorubicin (1-1,000 ng/ml) for 24 h after incubation with Exo-MG63/DXR (100 μg/ml) for 48 h. MG63 viability was affected by doxorubicin in a dose-dependent way and the resistance of doxorubicin for MG63 cells was increased following incubation with Exo-MG63/DXR (Fig. 2B). In particular, MG63 cells showed a significant increase in viability after exposed to 100 ng/ml of doxorubicin compared with other concentration of doxorubicin following incubation with Exo-MG63/DXR (Fig. 2C). However, the invasion of MG63 cells was significantly inhibited and the migration of MG63 cells was not affected by the Dox-MG63-Exo while the invasion and migration of MG63 cells was significantly inhibited at the same time following treatment with doxorubicin (Fig. 2D-F).

MG63 expressed MDR-1 mRNA after incubation with Exo-MG63/DXR. The expression of MDR-1 was evaluated by RT-qPCR after extracting total RNA from Exo-MG63/DXR, exosomes of MG63 (Exo-MG63) and their cells of origin. Exo-MG63/DXR expressed higher levels of MDR-1 mRNA compared with Exo-MG63. In addition, the expression of MDR-1 mRNA in Exo-MG63/DXR was significantly higher compared with that in MG63 cells (Fig. 2G). In addition, following incubation with Exo-MG63/DXR, the treated MG63 cells expressed higher levels of MDR-1 mRNA compared with the untreated MG63 cells (Fig. 2H). As expected, there was no difference in the expression of MDR-1 mRNA in the MG63 cells incubated with Exo-MG63.

Sequence and bioinformatic analysis of exosomal miRNAs. According to the analysis of the miRNA sequence of exosomes from MG63 cells and MG63/DXR cells, 2864 differentially expressed exo-miRNAs were detected and 456 miRNAs were upregulated and 98 miRNAs were downregulated significantly (fold-change>2.0, $P<5x10^{-2}$ and FDR<0.05; Fig. 3A-C). The 10 most up- and downregulated exo-miRNAs are shown in Table II. The related exo-miRNAs and pathways involved in the doxorubicin resistance for OS cells were identified by bioinformatic analysis (Fig. 3D-E). As a result, 20 high-risk pathways were found according to the KEGG analysis. Among them, pathways in cancer ($P=1.77x10^{-9}$), PI3K-Akt signaling pathway ($P=1.94x10^{-5}$), proteoglycans in cancer ($P=2.06x10^{-9}$), Rap1 signaling pathway ($P=4.86x10^{-3}$), Ras signaling pathway ($P=1.71x10^{-7}$) and regulation of actin cytoskeleton ($P=1.26x10^{-5}$) were the most prominent pathways enriched in quantiles with different exo-miRNAs in

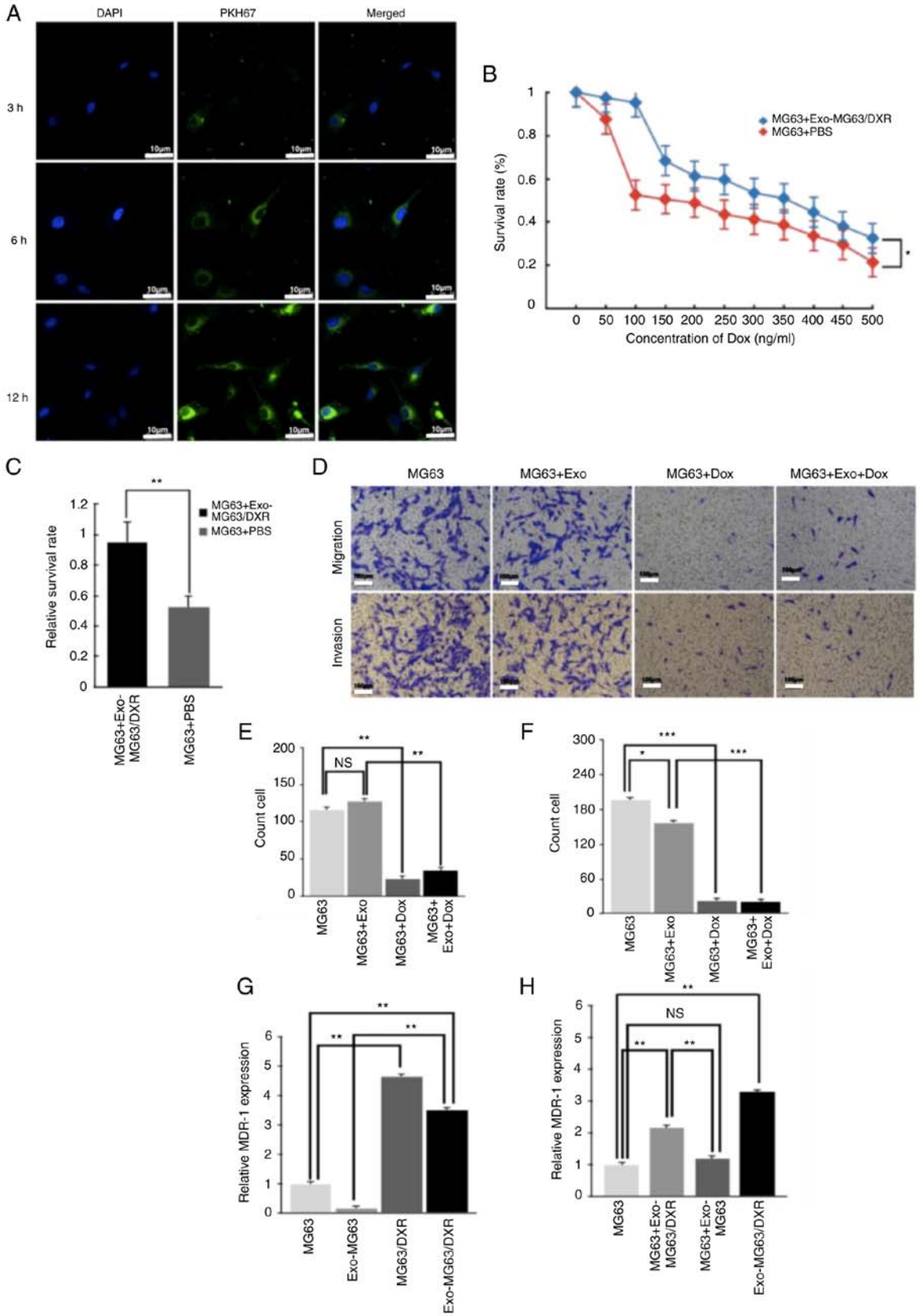

Figure 2. The influence of Exo-MG63/DXR for MG63 cells in the proliferation, migration and expression of MDR-1 after treated by doxorubicin. (A) PKH67 (Green) labelled Dox-MG63-Exo was taken up by MG63 cells after incubation for 3, 6 and 12 h. (B and C) Doxorubicin affected the MG63 viability in a dose-dependent way and Dox-MG63-Exo decreased the sensitivity of MG63 cells to doxorubicin. In particular, the sensitivity of MG63 cells was decreased most significantly with the concentration of doxorubicin at 100 ng/ml after incubation of Dox-MG63-Exo. (D-F) The invasion of MG63 cells was significantly inhibited after incubation with Dox-MG63-Exo, but the migration of MG63 cells was not affected by the Dox-MG63-Exo although the invasion and migration of MG63 cells was significantly inhibited at the same time after treated by doxorubicin. (G) Exo-MG63/DXR expressed higher levels of MDR-1 mRNA compared with Exo-MG63 and the expression of MDR-1 mRNA in Exo-MG63/DXR has significantly higher levels compared with MG63 cells. (H) MG63 cells expressed higher levels of MDR-1 mRNA following incubation with Exo-MG63/DXR and there was no difference of the expression of MDR-1 mRNA for the MG63 cells incubated with Exo-MG63. *P<0.05, **P<0.01 and ***P<0.001. Exo, exosomal; NS, not significant.

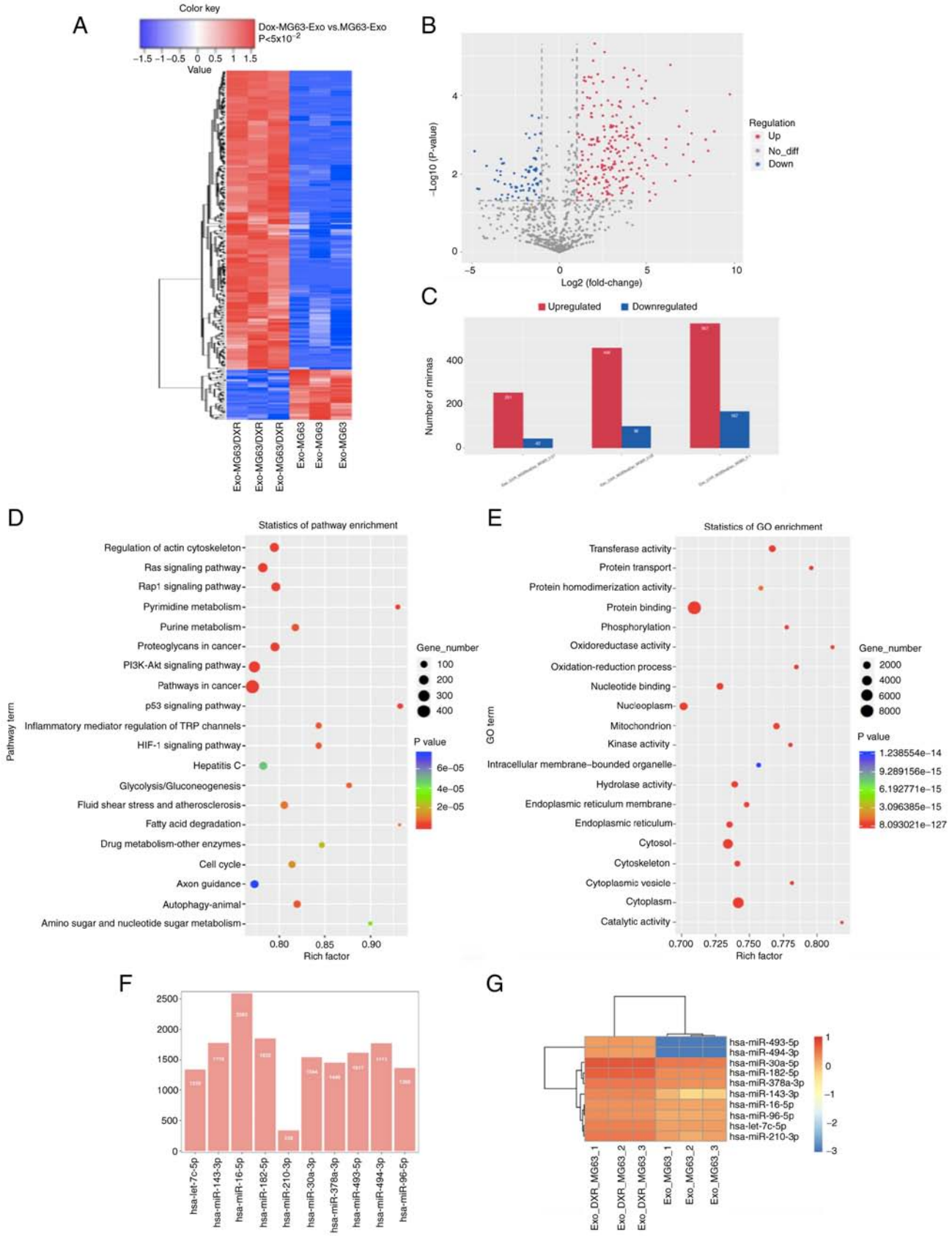

Figure 3. Exosomal miRNA sequence and bioinformatic analysis of exosomal miRNAs. (A) Heatmap of different exosomal miRNA profiles in MG63/DXR and MG63 cell lines. (B) Volcano map for exosomal miRNAs of the two cell lines according to the results of exo-miRNA sequence. (C) Among the exosomal miRNAs, 456 were upregulated and 98 were downregulated significantly (fold-change>2.0, P<0.05 and FDR<0.05) in exosomes. (D and E) Bioinformatic analysis of the exo-miRNAs by KEGG and GO enrichment. Pathways in cancer, PI3K-Akt signaling pathway, Proteoglycans in cancer, Rap1 signaling pathway, Ras signaling pathway and Regulation of actin cytoskeleton were the most prominent pathways enriched in quantiles with different exo-miRNAs in MG63/DXR cells. The protein binding, membrane, cytosol and cytoplasm were the prominent GO terms for the different expressed exo-miRNAs in MG63/DXR and MG63 cells. (F) Number of the target genes and (G) heatmap for the 10 randomly selected exosomal miRNAs. miRNA, microRNA; KEGG, Kyoto Encyclopedia of Genes and Genomes; GO, Gene Ontology; Exo, exosomal.

Table II. Ten most up- and downregulated exo-miRNAs.

miR name	miR sequence	Regulation	Fold change	P-values
hsa-miR-494-3p	TGAAACATACACGGGAAACCTCT	Up	inf	$8.53x10^{-4}$
hsa-miR-493-5p	TTGTACATGGTAGGCTTTCATT	Up	inf	$1.06x10^{-3}$
hsa-let-7c-5p	TGAGGTAGTAGGTTGTATGGTT	Up	4.05	$4.86x10^{-6}$
hsa-miR-210-3p	CTGTGCGTGTGACAGCGGCTGA	Up	8.57	$3.84x10^{-5}$
hsa-miR-182-5p	TTTGGCAATGGTAGAACTCACACCG	Up	8.04	$1.76x10^{-4}$
hsa-miR-30a-5p	TGTAAACATCCTCGACTGGAAGCT	Up	5.30	$1.79x10^{-4}$
hsa-miR-25-3p	CATTGCACTTGTCTCGGTCTGA	Up	5.58	$3.27x10^{-4}$
hsa-miR-143-3p	TGAGATGAAGCACTGTAGCTC	Up	24.20	$5.21x10^{-4}$
hsa-miR-183-5p	TATGGCACTGGTAGAATTCACT	Up	7.53	$6.43x10^{-4}$
hsa-miR-34c-5p	AGGCAGTGTAGTTAGCTGATTGC	Up	190.42	$9.40x10^{-4}$
hsa-miR-199a-5p_R-1	CCCAGTGTTCAGACTACCTGTT	Down	0.44	$2.19x10^{-3}$
hsa-miR-152-3p	TCAGTGCATGACAGAACTTGG	Down	0.42	$2.59x10^{-3}$
hsa-miR-185-5p	TGGAGAGAAAGGCAGTTCCTGA	Down	0.39	$4.00x10^{-3}$
hsa-miR-23a-3p_R-1	ATCACATTGCCAGGGATTTC	Down	0.33	$6.58x10^{-3}$
hsa-miR-16-2-3p_L+1R-1	ACCAATATTACTGTGCTGCTTT	Down	0.30	$8.30x10^{-3}$
hsa-miR-27a-3p_R-1	TTCACAGTGGCTAAGTTCCG	Down	0.31	$8.95x10^{-3}$
hsa-miR-24-3p_R-2	TGGCTCAGTTCAGCAGGAAC	Down	0.49	$9.61x10^{-3}$
hsa-miR-146a-5p	TGAGAACTGAATTCCATGGGTT	Down	0.26	$1.25x10^{-2}$
hsa-miR-148a-3p	TCAGTGCACTACAGAACTTTGT	Down	0.08	$1.44x10^{-2}$
hsa-miR-423-5p	TGAGGGGCAGAGAGCGAGACTTT	Down	0.43	$1.79x10^{-2}$

miRNA/miR, microRNA.

MG63/DXR cells. In addition, according to the analysis of GO enrichment, protein binding, membrane, cytosol and cytoplasm were the prominent GO terms for the differentially expressed exo-miRNAs in MG63/DXR and MG63 cells.

Validation of different exosomal miRNAs confer doxorubicin resistance to OS cells. Based on the statistical significance and biological plausibility, 10 miRNAs, including miR-30a-5p, miR-16-5p, miR-96-5p, let-7c-5p, miR-182-5p, miR-210-3P, miR-378a-3P, miR-493-5p, miR-494-3p and miR-143-3p, were selected for validation from the exo-miRNA sequence by RT-qPCR in four OS cells including MG63 cells, MG63/DXR cells, KHOS cells and KHOS/DXR cells (Table III). The heatmap and the number of the target genes of the exo-miRNAs are shown in Fig. 3F and G. A total of 10 randomly exosomal miRNAs, including miR-30a-5p, miR-16-5p, miR-96-5p, let-7c-5p, miR-182-5p, miR-210-3P, miR-378a-3P, miR-493-5p, miR-494-3p and miR-143-3p, were selected for validation by TaqMan RT-qPCR in four OS cells. According to the result of RT-qPCR, the expression of miR-143-3p was significantly increased in exosomes from MG63/DXR cells and KHOS/DXR cells compared with MG63 cells and KHOS cells and miR-493-5p and miR-494-3p were the two most significantly differentially expressed miRNAs between MG63 cells and MG63/DXR cells (Fig. 4A-J). To investigate the function of the three exo-miRNAs in OS cells, MG63 cells and KHOS cells were infected with lentiviral vectors expressing mimic of exosomal miR-143-3p, miR-493-5p and miR-494-3p and the MG63/DXR cells and KHOS/DXR cells were infected with lentiviral vectors expressing inhibitor of the three miRNAs. The negative control mimic and inhibitor of the three miRNAs were used as negative controls (NC). The transfection for each of the three miRNA mimics in MG63 cells and KHOS cells and inhibitors in MG63/DXR cells and KHOS/DXR cells are shown separately in Fig. 5A-L. After 48 h of incubation of the infected exosomes, the four OS cells were treated with doxorubicin (100 ng/ml) for another 24 h (Fig. 5M-P). The results of cell viability evaluated by CellTiter-Glo indicated that exosomal miR-143-3p mimic significantly increased the doxorubicin resistance for the MG63 cells and KHOS cells compared with the NC group while the exosomal miR-493-5p mimic and exosomal miR-494-3p mimic did not perform a similar function in the two OS cell lines. In addition, the exosomal miR-143-3p inhibitor reduced the doxorubicin resistance for the MG63/DXR cells and KHOS/DXR cells according to the result of cell viability compared with the NC group (Fig. 5M-P). As a result, the present study found upregulation of exosomal miR-143-3p led to poor chemotherapeutic response to osteosarcoma, highlighting the importance of miR-143-3p as an oncogene in chemotherapy for osteosarcoma.

Discussion

Multidrug resistance (MDR) is a major concern regarding the clinical management of osteosarcoma patients and a key issue in the failure of current treatment (4). Exosomes have been reported to serve an increasingly important role in different stages of tumor progression and chemotherapy resistance (5-7). The present study reported that exosomes derived from doxorubicin-resistant OS cells are able to transfer phenotypic

Table III. Ten randomly selected miRNAs for validation from exo-miRNA sequence by TaqMan reverse transcription-quantitative PCR.

miR name	miR sequence	Regulation	Fold change	P-values	KEGG name	GO name	GO function
miR-30a-5p	TGTAAACATCCTCGACTGG AAGCT	Up	5.30	$1.79x10^{-4}$	Pathways in cancer	Nucleoplasm	Cellular component
miR-16-5p	TAGCAGCACGTAAATATTG GCG	Up	2.55	$1.83x10^{-4}$	MicroRNAs in cancer	Nucleotide binding	Cellular component
miR-96-5p	TTTGGCACTAGCACATTTT TGCT	Up	3.83	$1.32x10^{-5}$	MicroRNAs in cancer	Nucleoplasm	Cellular component
let-7c-5p	TGAGGTAGTAGGTTGTATG GTT	Up	4.05	$4.86x10^{-6}$	MicroRNAs in cancer	Nucleoplasm	Cellular component
miR-182-5p	TTTGGCAATGGTAGAACTC ACACCG	Up	8.04	$1.76x10^{-4}$	Hippo signaling pathway	Nucleoplasm	Cellular component
miR-210-3P	CTGTGCGTGTGACAGCGG CTGA	Up	8.57	$3.84x10^{-5}$	Ras signaling pathway	Nucleoplasm	Cellular component
miR-378a-3P	ACTGGACTTGGAGTCAGA AGGC	Up	3.56	$3.47x10^{-5}$	Ras signaling pathway	Protein binding	Molecular function
miR-493-5p	TTGTACATGGTAGGCTTTC ATT	Up	inf	$1.06x10^{-3}$	p53 signaling pathway	Protein binding	Molecular function
miR-494-3p	TGAAACATACACGGGAAA CCTCT	Up	inf	$8.53x10^{-4}$	Proteoglycans in cancer	Protein binding	Molecular function
miR-143-3p	TGAGATGAAGCACTGTAG CTC	Up	24.20	$5.21x10^{-4}$	Pathways in cancer	Protein binding	Molecular function

miRNA/miR, microRNA; KEGG, Kyoto Encyclopedia of Genes and Genomes; GO, Gene Ontology.

characteristics to doxorubicin-sensitive OS cells. According to the results of exo-miRNA sequence and bioinformatic analysis of the differentially expressed exo-miRNAs from doxorubicin-resistant OS cells and doxorubicin-sensitive OS cells, the present study found a substantial profile of exo-miRNAs was differentially expressed in OS cell lines with different chemotherapeutic response. Notably, the results for validation of different exosomal miRNAs by RT-qPCR indicated that the expression level of miR-143-3p was significantly different in the exosomes of OS cell lines with different chemotherapeutic responses and upregulation of exosomal miRNA-143-3p abundance can induce a poor chemotherapeutic response in OS cells. These results could help monitor or predict disease progression during chemotherapeutic treatment of OS.

Exosomes facilitate cell-cell crosstalk within the tumor environment, which serves a crucial role in augmenting MDR pathways (12,13). Santos *et al* (14) report that breast cancer stem cells and doxorubicin- and paclitaxel-resistant breast cells can secrete more exosomes than parental cells. Fang *et al* (15) found that liver cancer cells with high metastatic potential secreted more exosomes than those with low metastatic potential. The above findings are consistent with the findings of the present study that doxorubicin-resistant OS cells release more exosomes than doxorubicin-sensitive OS cells. The phenomenon that exosomes released by drug resistant cells can mediate the acquired MDR of drug-sensitive cancer cells is observed in ovarian cancer (16), prostate cancer (17), breast cancer (18) and melanoma (19). In the present study, this phenomenon was also observed in OS cells, including the capacity for doxorubicin resistance and the presence of selective MDR-1 mRNA, except for the invasion and migration of OS cells, which need further investigation in the future.

A number of studies have identified that exosomes have the ability to transport molecular information such as proteins, mRNAs and miRNAs from one cell to another to induce chemoresistance and malignant phenotypic traits (20-23). Exosomal miR-126a, miR-222-3p, miR-32-5p and miR-222 are reported to be involved in the MDR of malignant tumors (20-23). The present study provided the first results of the miRNA sequence for different exosomal miRNAs expression in doxorubicin-sensitive and doxorubicin-resistant OS cells. In addition, according to the results of bioinformatic analysis and validation of differential exosomal miRNAs, a substantial profile of different expressed exosomal miRNAs was found in OS cell lines with different chemotherapeutic response.

miR-143 is located on human chromosome 5. Depending on the different site of cleavage, the stem-loop structure of miR-143 precursor can form miR-143-3p and miR-143-5p (24). Previous reports indicate that the expression levels of miR-143 is associated with clinical stage, disease grade and lymph node metastasis (25,26). Regulating the expression of miR-143-3p inhibits or promotes the cell proliferation, migration and

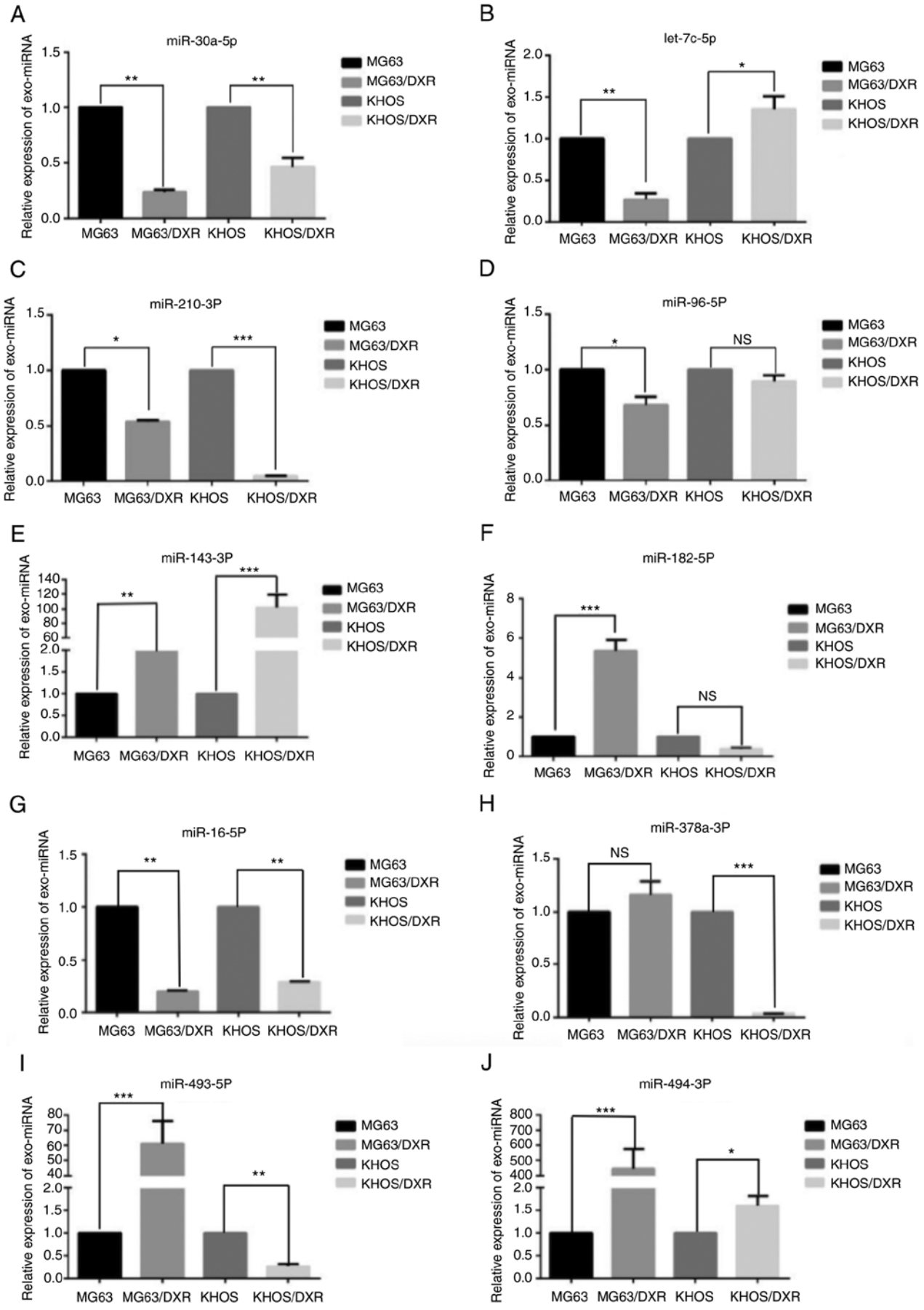

Figure 4. Validation of different exo-miRNAs confer doxorubicin resistance to OS cells by RT-qPCR. A total of 10 randomly exosomal miRNAs, including (A) miR-30a-5p, (B) let-7c-5p, (C) miR-210-3P, (D) miR-96-5p, (E) miR-143-3p, (F) miR-182-5p, (G) miR-16-5p, (H) miR-378a-3P, (I) miR-493-5p and (J) miR-494-3p were selected for validation by TaqMan RT-qPCR in four OS cells. *P<0.05, **P<0.01 and ***P<0.001. miRNA, microRNA; OS, osteosarcoma; RT-qPCR, reverse transcription-quantitative PCR; NS, not significant.

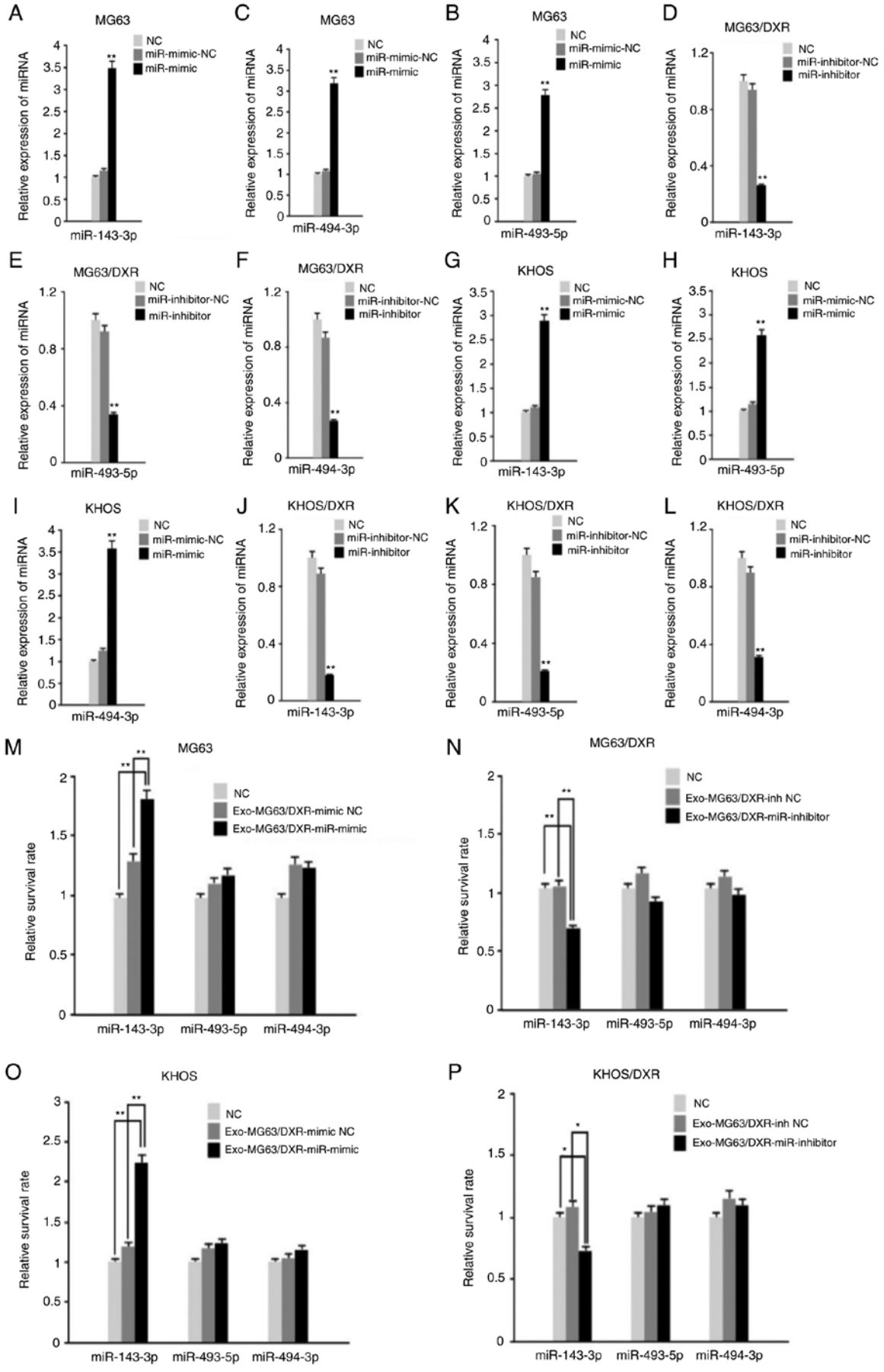

Figure 5. The transfection for each of the three miRNA mimics in MG63 cells and KHOS cells and inhibitors in MG63/DXR cells and KHOS/DXR cells (A-L) and the results of cell viability evaluated by CTG following infection of MG63 cells and KHOS cells with lentiviral vectors expressing mimic of exosomal miR-143-3p, miR-493-5p and miR-494-3p. (M and N) MG63/DXR cells and (O and P) KHOS/DXR cells were infected with lentiviral vectors expressing inhibitor of the three miRNAs. miRNA, microRNA; CTG, CellTiter-Glo; Exo, exosomal; *P<0.05 and **P<0.01.

invasion in hepatocellular carcinoma and triple negative breast cancer (27,28). The expression level of miR-143-3p is significantly decreased for OS cells and serum of OS patients (29). The present study was the first, to the best of the authors' knowledge, to report on the expression of exosomal miR-143-3p for OS cells with different chemotherapeutic response. It was found that miR-143-3p was highly expressed in exosomes from doxorubicin-resistant OS cells and that upregulation of exosomal miR-143-3p abundance can induce a poor chemotherapeutic response to osteosarcoma, highlighting the importance of miR-143-3p as an oncogene in osteosarcoma and providing new insights into chemotherapy for osteosarcoma. In 2005, Zhang *et al* (30) reported that forced miR-143 expression significantly reversed chemoresistance, which was different from the result of the present study. However, the present study investigated the miRNAs which could be stably present in exosomes and the expression level of miRNA-143 may be different in the exosomes and OS cells; the present study focused on the function of exosomal miRNA in chemoresistance in OS cells. Furthermore, depending on the different site of cleavage, the stem-loop structure of miR-143 precursor can form miR-143-3p and miR-143-5p (29). The present study studied the function of exosomal miRNA143-3p in the chemoresistance of OS cells and exosomal miR-143-3p induced the doxorubicin-resistant phenotype according to the PI3K/mTOR pathway and the key protein in this pathway will be reported in the future.

There are some limitations to the present study. First, multivariate analysis, such as Fisher discriminant analysis, could be further applied to explore the differential role of miRNAs in the chemotherapeutic response. Second, animal experiments need to be conducted to support the conclusion of the present study. Last but not least, the investigation of the different samples from different OS patients, such as serum of the patients and the specimen of the osteosarcoma, need to be performed to prove the results of the present study.

To conclude, the present study corroborated the evidence that exosomes from doxorubicin-resistant osteosarcoma cells are capable of transferring chemoresistant phenotypic traits and MDR-1, a specific mRNA of chemoresistance. In addition, it revealed a substantial abundance of differentially expressed miRNAs present in the exosomes from OS cells with the different chemotherapeutic response. Importantly, the present study found that the upregulation of exosomal miR-143-3p abundance was associated with poor chemotherapeutic response to osteosarcoma cells, which was highly expressed in doxorubicin-resistant OS cells, highlighting the importance of miR-143-3p as an oncogene in osteosarcoma; this may provide new insights into chemotherapy of osteosarcoma.

Acknowledgements

Not applicable.

Funding

The present study was supported by grants from the National Natural Science Foundation of China (grant nos. 81872174 and 82072963), Program of Shanghai Academic Research Leader (grant no. 19XD1402900) and Program of Shanghai Sailing Program (grant no. 20YF1437700).

Availability of data and materials

The datasets used and/or analyzed during the current study are available from the corresponding author on reasonable request.

Authors' contributions

TC contributed to the conception and design of the study, analysis and interpretetion of the data. TZ contributed to the drafting of the manuscript and acquisition of data. CZ contributed to the design of the study, gave final approval of the version to be published and agreed to be accountable for all aspect of work. TC and CZ confirm the authenticity of all the raw data. All authors read and approved the final manuscript.

Ethics approval and consent to participate

The the study was approved by the Institutional Review Board of Tongji University (Shanghai, China) and was performed in accordance with the ethical standards prescribed by the Helsinki Declaration.

Patient consent for publication

Not applicable.

Competing interests

The authors declare that they have no competing interests.

Authors' information

Tao Cai was an undergraduate medical student in the Department of Orthopedic Surgery, Shanghai Tenth People's Hospital Affiliated To Tongji University when the article was submitted. Now, Dr Tao Cai is a surgeon of the Department of Orthopedic Surgery, Tongji Hospital Affiliated to Tongji University.

References

1. Miller RW: Contrasting epidemiology of childhood osteosarcoma, Ewing's tumor, and rhabdomyosarcoma. Natl Cancer Inst Monogr 56: 9-15, 1981.
2. Ottaviani G and Jaffe N: The Epidemiology of Osteosarcoma. Cancer Treat Res 152: 3-13, 2009.
3. Provisor AJ, Ettinger LJ, Nachman JB, Krailo MD, Makley JT, Yunis EJ, Huvos AG, Betcher DL, Baum ES, Kisker CT and Miser JS: Treatment of nonmetastatic osteosarcoma of the extremity with preoperative and postoperative chemotherapy: A report from the Children's Cancer Group. J Clin Oncol 15: 76-84, 1997.
4. Gianferante DM, Mirabello L and Savage SA: Germline and somatic genetics of osteosarcoma-connecting aetiology, biology and therapy. Nat Rev Endocrinol 13: 480-491, 2017.
5. Milane L, Singh A, Mattheolabakis G, Suresh M and Amiji MM: Exosome mediated communication within the tumor microenvironment. J Control Release 219: 278-294, 2015.
6. Teng X, Chen L, Chen W, Yang J, Yang Z and Shen Z: Mesenchymal stem cell-derived exosomes improve the microenvironment of infarcted myocardium contributing to angiogenesis and anti-inflammation. Cell Physiol Biochem 37: 2415-2424, 2015.
7. Baixauli F, López-Otín C and Mittelbrunn M: Exosomes and autophagy: Coordinated mechanisms for the maintenance of cellular fitness. Front Immunol 5: 403, 2014.

8. Nair R, Santos L, Awasthi S, von Erlach T, Chow LW, Bertazzo S and Stevens MM: Extracellular vesicles derived from preosteoblasts influence embryonic stem cell differentiation. Stem Cells Dev 23: 1625-1635, 2014.
9. Tkach M and Théry C: Communication by extracellular vesicles: Where we are and where we need to go. Cell 164: 1226-1232, 2016.
10. Zhao L, Liu W, Xiao J and Cao B: The role of exosomes and 'exosomal shuttle microRNA' in tumorigenesis and drug resistance. Cancer Lett 356 (2 Pt B): 339-346, 2015.
11. Livak KJ and Schmittgen TD: Analysis of relative gene expression data using real-time quantitative PCR and the 2(-Delta Delta C(T)) method. Methods 25: 402-408, 2001.
12. Chen WX, Liu XM, Lv MM, Chen L, Zhao JH, Zhong SL, Ji MH, Hu Q, Luo Z, Wu JZ and Tang JH: Exosomes from drug-resistant breast cancer cells transmit chemoresistance by a horizontal transfer of microRNAs. PLoS One 9: e95240, 2014.
13. Robbins PD and Morelli AE: Regulation of immune responses by extracellular vesicles. Nat Rev Immunol 14: 195-208, 2014.
14. Santos JC, Lima NDS, Sarian LO, Matheu A, Ribeiro ML and Derchain SFM: Exosome-mediated breast cancer chemoresistance via miR-155 transfer. Sci Rep 8: 829, 2018.
15. Fang T, Lv H, Lv G, Li T, Wang C, Han Q, Yu L, Su B, Guo L, Huang S, *et al*: Tumor-derived exosomal miR-1247-3p induces cancer-associated fibroblast activation to foster lung metastasis of liver cancer. Nat Commun 9: 191, 2018.
16. Safaei R, Larson BJ, Cheng TC, Gibson MA, Otani S, Naerdemann W and Howell SB: Abnormal lysosomal trafficking and enhanced exosomal export of cisplatin in drug-resistant human ovarian carcinoma cells. Mol Cancer Ther 4: 1595-1604, 2005.
17. Corcoran C, Rani S and O'Driscoll L: miR-34a is an intracellular and exosomal predictive biomarker for response to docetaxel with clinical relevance to prostate cancer progression. Prostate 74: 1320-1334, 2014.
18. Lv MM, Zhu XY, Chen WX, Zhong SL, Hu Q, Ma TF, Zhang J, Chen L, Tang JH and Zhao JH: Exosomes mediate drug resistance transfer in MCF-7 breast cancer cells and a probable mechanism is delivery of P-glycoprotein. Tumour Biol 35: 10773-10779, 2014.
19. Federici C, Petrucci F, Caimi S, Cesolini A, Logozzi M, Borghi M, D'Ilio S, Lugini L, Violante N, Azzarito T, *et al*: Exosome release and low pH belong to a framework of resistance of human melanoma cells to cisplatin. PLoS One 9: e88193, 2014.
20. Yu D, Wu Y, Zhang X, Lv MM, Chen WX, Chen X, Yang SJ, Shen H, Zhong SL, Tang JH and Zhao JH: Exosomes from adriamycin-resistant breast cancer cells transmit drug resistance partly by delivering miR-222. Tumour Biol 37: 3227-3235, 2016.
21. Deng Z, Rong Y, Teng Y, Zhuang X, Samykutty A, Mu J, Zhang L, Cao P, Yan J, Miller D and Zhang HG: Exosomes miR-126a released from MDSC induced by DOX treatment promotes lung metastasis. Oncogene 36: 639-651, 2017.
22. Wei F, Ma C, Zhou T, Dong X, Luo Q, Geng L, Ding L, Zhang Y, Zhang L, Li N, *et al*: Exosomes derived from gemcitabine-resistant cells transfer malignant phenotypic traits via delivery of miRNA-222-3p, Mol Cancer 16: 132, 2017.
23. Fu X, Liu M, Qu S, Ma J, Zhang Y, Shi T, Wen H, Yang Y, Wang S, Wang J, *et al*: Exosomal microRNA-32-5p induces multidrug resistance in hepatocellular carcinoma via the PI3K/Akt pathway. J Exp Clin Cancer Res 37: 52, 2018.
24. Sun X, Dai G, Yu L, Hu Q, Chen J and Guo W: miR-143-3p inhibits the proliferation, migration and invasion in osteosarcoma by targeting FOSL2. Sci Rep 8: 606, 2018.
25. Wang H, Li Q, Niu X, Wang G, Zheng S, Fu G and Wang Z: miR-143 inhibits bladder cancer cell proliferation and enhances their sensitivity to gemcitabine by repressing IGF-1R signaling. Oncol Lett 13: 435-440, 2017.
26. Wang L, He J, Xu H, Xu L and Li N: MiR-143 targets CTGF and exerts tumour-suppressing functions in epithelial ovarian cancer. Am J Transl Res 8: 2716-2726, 2016.
27. Chen L, Yao H, Wang K and Liu X: Long non-coding RNA MALAT1 regulates ZEB1 expression by sponging miR-143-3p and promotes hepatocellular carcinoma progression. J Cell Biochem 118: 4836-4843, 2017.
28. Li D, Hu J, Song H, Xu H, Wu C, Zhao B, Xie D, Wu T, Zhao J and Fang L: miR-143-3p targeting LIM domain kinase 1 suppresses the progression of triple-negative breast cancer cells. Am J Transl Res 9: 2276-2285, 2017.
29. Yang L, Li H and Huang A: MiR-429 and MiR-143-3p function as diagnostic and prognostic markers for osteosarcoma. Clin Lab 66 2020.
30. Zhou J, Wu S, Chen Y, Zhao J, Zhang K, Wang J and Chen S: microRNA-143 is associated with the survival of ALDH1+CD133+ osteosarcoma cells and the chemoresistance of osteosarcoma. Exp Biol Med (Maywood) 240: 867-875, 2015.